Materials Transactions, Vol. 44, No. 12 (2003) pp. 2617 to 2624

Microstructure and Mechanical Properties of Strip Cast Al-Mg-Si-X Alloys

Young S. Park, Sang B. Lee and Nack J. Kim

Center for Advanced Aerospace Materials, Pohang University of Science and Technology, Pohang 790-784, Korea

A study has been conducted on the microstructure and mechanical properties of strip cast Al6061 alloy with and without a 0.5 mass% Mn addition. The microstructures of the as-cast alloys are characterized by the presence of Si particles (<1 μm) and clusters of fine α-AlFeSi particles (<50 nm) along grain boundaries. In addition, there is the development of well-defined subgrains caused by the effects of hot rolling during strip casting. By T6 heat treatment, Si particles along grain boundaries are replaced by fine α-AlFeSi particles. There is also a formation of α-AlFeSi particles within the Al matrix by heat treatment. The addition of Mn results in an increase in the volume fraction of α-AlFe(Mn)Si particles within the Al matrix, which is associated with a corresponding decrease in the volume fraction of Mg_2Si precipitates within the Al matrix over that observed in the base alloy. Accordingly, the Mn containing alloy shows a lower yield strength but a higher ultimate tensile strength due to a greater work hardening rate than the base alloy. The increased work hardening rate of the Mn containing alloy is due to the presence of uniformly distributed fine α-AlFe(Mn)Si particles within the Al matrix. The present study shows that strip casting is a viable process for the fabrication of structural Al alloys.

(Received August 27, 2003; Accepted October 10, 2003)

Keywords: *strip casting, 6061 Al alloy, AlFeSi*

1. Introduction

Direct chill (DC) casting has been the most important casting technique for producing large rolling slabs and extrusion billets of Al alloys. At the same time, continuous casting techniques for Al alloy products have been available for 50 years. There are various types of continuous casters for producing Al alloy products; for example, the Hazelett twin-belt caster, which uses mild steel belts and fast film water cooling, or the Hunter twin-roll caster, which uses two water-cooled steel rolls, to produce strip. Currently, twin-roll casting or strip casting is the preferred method for fabricating thin-gauge Al sheets and foils.[1] One of the main advantages of strip casting is that capital investment for a strip caster is much lower than the conventional ingot/hot rolling process. Since the strip casting process combines solidification and hot rolling into one operation, the hot rolling needed for conventionally produced ingots can be eliminated or reduced, resulting in substantial savings in energy and cost. Besides these economic benefits, strip casting is also able to reduce segregation, to improve inclusion size distribution and to refine microstructural and textural homogeneity.[2–5] In fact, the steel industry is quite enthusiastic about strip casting and several R&D efforts are currently under way to produce steels with high solute contents such as stainless steels by strip casting.[6–11] However, the application of strip casting in non-ferrous alloys such as Al and Mg alloys is largely limited to alloys with low solute contents.[12–14]

Recently, attempts have been made to fabricate the highly alloyed Al-6Fe-1V-2Si alloy by strip casting using a single-roll caster.[15–17] Al-6Fe-1V-2Si alloy is a derivative of the commercial non-heat treatable Al8009 alloy. Al8009 alloy derives its excellent high temperature properties from a uniform distribution of fine, thermally stable dispersoids,[18] which is a consequence of the rapid solidification/powder metallurgy (RS/PM) process used to produce the alloy. The previous studies on strip casting of the Al-6Fe-1V-2Si alloy showed that its microstructure is less than desirable since it has a coarser microstructure than that of the RS/PM alloy. However, these studies also showed that otherwise non-existing metastable phases form in the microstructure of the strip due to the fast solidification rate associated with strip casting, suggesting that strip casting can be applied to the production of relatively highly alloyed Al alloys.

The present research was aimed at studying the structure and properties of strip cast SC6061 alloy to establish the feasibility of strip casting for the production of Al alloys with modest solute contents. In addition to the base Al6061 alloy, the same alloy containing an addition of 0.5 mass% Mn was also studied to utilize the potentially beneficial effect of Mn on the formation of dispersoids.

2. Experimental Procedure

The strip casting apparatus is shown schematically in Fig. 1. Molten metal is fed from the melting furnace through the tundish into the gap between two water-cooled rolls. The rolls are made of Cu-0.7 mass%Be and are 200 mm in diameter and 100 mm in width. The roll speed can be varied

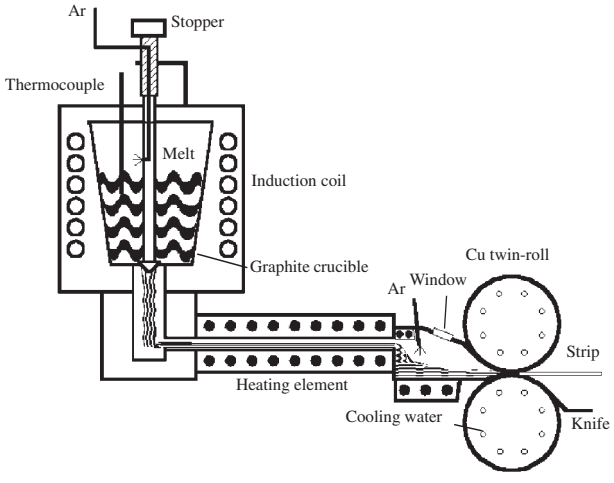

Fig. 1 Schematic drawing of the twin roll caster used in the present study.

Table 1 Chemical compositions (mass%) of the alloys used in the present study

	Al	Mg	Si	Mn	Fe
SC6061	Bal.	0.89	0.50	0.06	0.43
SC6061Mn	Bal.	0.90	0.49	0.54	0.40

continuously in the range of 4–16 m/min. Two alloys have been strip cast in the present study; Al6061 with and without 0.5 mass% Mn addition (SC6061Mn and SC6061, respectively) and their chemical compositions are shown in Table 1. These alloys were induction melted in an Ar atmosphere at 1000°C and transferred into a tundish maintained at a temperature of 750°C. The roll gap was set at 2 mm and the roll speed was 4 m/min, 8 m/min or 16 m/min. The strips produced were 2 mm in thickness and 50–70 mm in width.

Microstructural observation of the strip was conducted on the cross sections by optical microscopy (OM) and scanning electron microscopy (SEM). Details of the microstructural constituents were analyzed on longitudinal sections by transmission electron microscopy (TEM). Thin foils for TEM were made by ion milling to prevent the formation of oxygen related artifacts. Strips were subjected to a solution treatment at 540°C for 2 hours followed by aging at temperatures ranging from 170 to 210°C for 2 hours. Vickers microhardness tests were conducted on the cross sections with an applied load of 300 g. Tensile tests were conducted using flat tensile specimens with a 12.6 mm gage length, 2 mm gage thickness and 5 mm gage width and a strain rate of $8 \times 10^{-5}\ s^{-1}$. Reported tensile properties are the averages of at least 3 test results.

3. Results and Discussion

3.1 Effect of processing variables

To understand the effects of the processing variables on the microstructure of the strip, several combinations of processing variables have been used to cast strips. Figs. 2(a) and (b) are cross sectional optical micrographs of strips cast with a roll gap of 2 mm and roll speeds of 16 m/min and 8 m/min, respectively. It shows that the degree of central segregation increases as roll speed increases. Energy dispersive X-ray spectroscopy (EDS) analysis shows that the central segregation is mostly due to Fe, which is one of the most common impurities in Al alloys. In the case of single roll casting such as melt spinning, an increase in roll speed results in a decrease in strip thickness accompanied by an increase in solidification rate. On the other hand, twin roll casting results in the same strip thickness if the same roll gap is used during casting. In the case of a fast roll speed, the mid-thickness area of the strip can still be liquid or in a semi-solid state when the strip exits the roll gap. In such cases, the mid-thickness area of the strip experiences a much slower solidification rate resulting in central segregation. When the roll speed is slow, however, the strip can completely be solidified before it passes through the rolls. Moreover, the solidified strip receives a rolling deformation, which might result in improved microstructural characteristics. A further decrease in the roll speed to 4 m/min results in the removal of central segregation as shown in Fig. 2(c). It also shows the presence

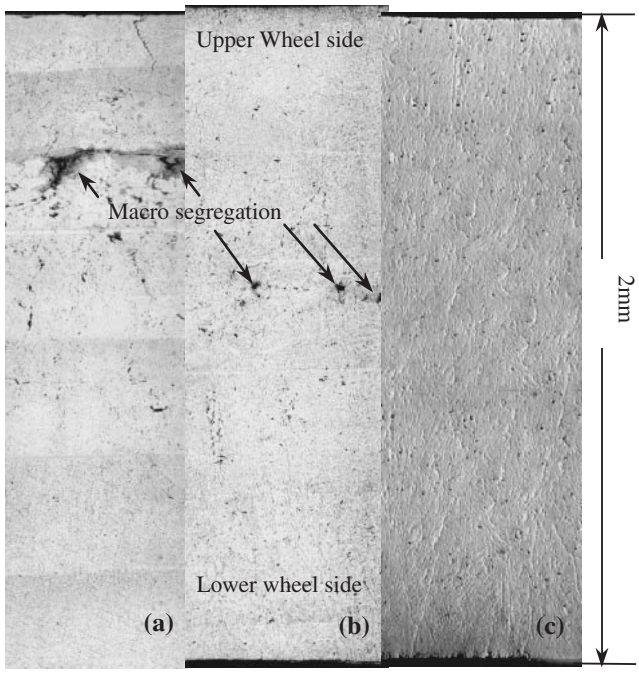

Fig. 2 Cross-sectional optical micrographs of as-cast SC6061 alloy processed with different roll speeds; (a) 16 m/min, (b) 8 m/min, and (c) 4 m/min.

of elongated structures through the thickness of strip and that the microstructure of such a strip is quite uniform through the thickness of the strip. Change in the roll gap at the same roll speed also has an effect on microstructure. It has been shown that, at any roll speed, increasing the roll gap results in the occurrence of central segregation and the relatively coarse cell structure in mid-thickness area of the strip. For example, the strip casting with roll speed of 4 m/min and roll gap of 3 mm results in the microstructure resembling that of the strip cast with roll speed of 8 m/min and roll gap of 2 mm (Fig. 2b). Strip castings with roll gap smaller than 2 mm generally result in the microstructures which have less degree of central segregation than the ones with larger rolling gaps. However, at the roll speed of 4 m/min, there is no appreciable difference in the microstructures between the strip cast with roll gap of 2 mm and the one with smaller roll gap. Similar behavior has been found for the SC6061Mn alloy.

The cooling rate for the strip casting has been estimated by using the experimental relationships between average cooling rate and dendrite arm or cell spacing available for aluminum alloys.[19] The cell spacing of the strips cast with roll gap of 2 mm has been measured to be $5 \sim 7\ \mu m$, giving the estimation of cooling rate to be around 1000°C/s irrespective of roll speed condition and alloys. This value is somewhat slower than that of rapid solidification but faster than that of DC casting.

3.2 Microstructure

3.2.1 As-cast microstructure

As shown above, the microstructure of the strip cast under optimum processing conditions is quite uniform through the thickness of the strip. Figures 3(a) and (b) are high magnification SEM micrographs of the central region of the SC6061 alloy strip cast with roll speed of 4 m/min and an

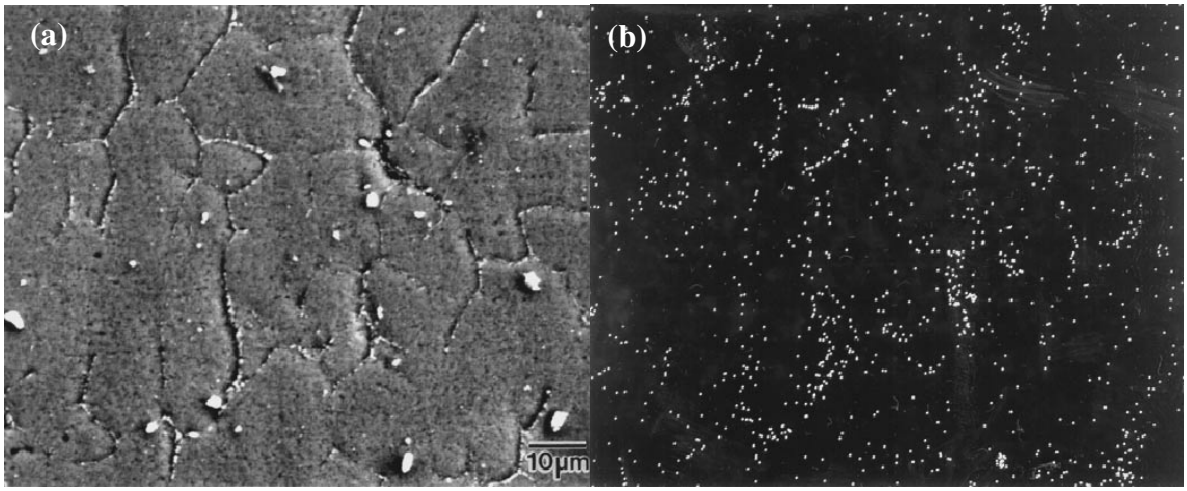

Fig. 3 SEM micrographs of as-cast SC6061 alloy showing the segregation of Si along grain boundaries; (a) SEM image and (b) X-ray mapped image.

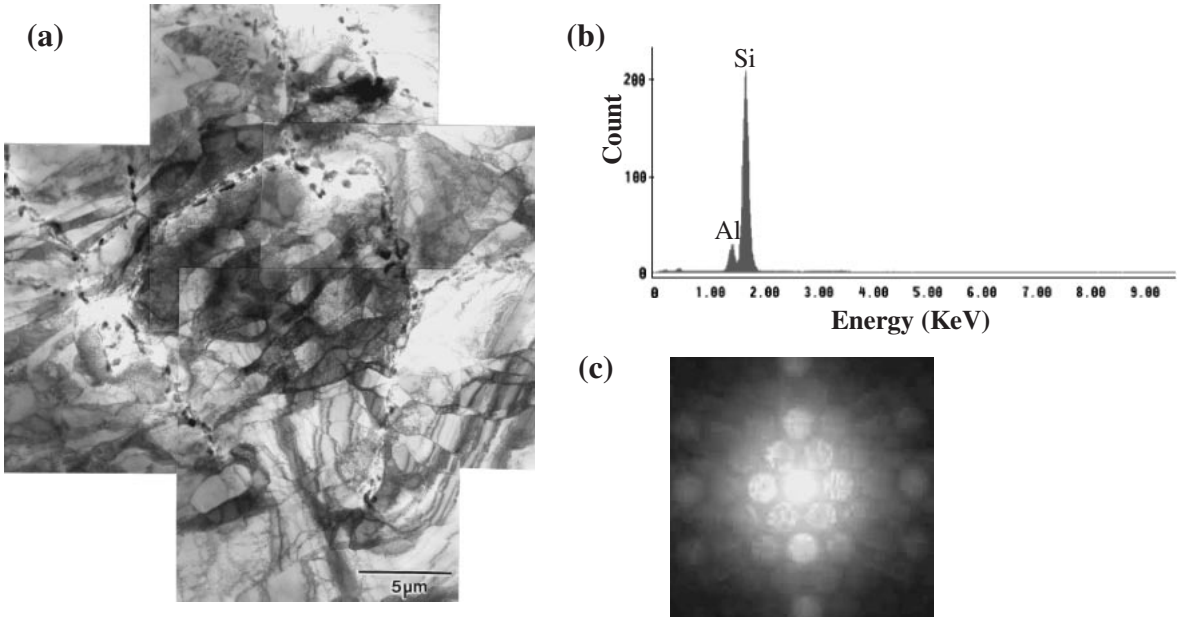

Fig. 4 (a) BF micrograph of as-cast SC6061 alloy, (b) EDS spectra from Si containing particles and (c) microdiffraction pattern of Si containing particles.

X-ray mapped image of Si, respectively. It shows that there are Si containing particles along the grain boundaries. To understand the detailed nature of these particles, TEM analysis has been conducted and the results are shown in Fig. 4. Bright field micrograph of Fig. 4(a) shows that the 200–300 nm sized elongated particles are present along the grain boundaries. EDS analysis shows that the particles mostly contain Si (Fig. 4b). It is not clear from the EDS analysis whether Al is present in the particles since Al peak can come from the surrounding matrix. Microdiffraction analysis of the particles shows that they have diamond cubic structure with $a = 0.5431$ nm (Fig. 4c), which is consistent with the particles being Si. Higher magnification micrograph of the grain boundary area shows that the clusters of fine particles (<50 nm) decorate the grain boundaries, in addition to the above mentioned Si particles which are the major phase (Fig. 5a). Selected area diffraction (SAD) from these particles results in incomplete ring patterns since the particles are small and their volume fraction is not large enough to give complete ring pattern as shown in Fig. 5(b). However, the ring pattern can be indexed as schematically shown in Fig. 5(c), indicating that they are a bcc phase. Its lattice parameter has been measured to be 1.258 nm. EDS analyses of these fine particles show that they contain Al, Si and Fe as shown in Fig. 5(d). This phase is identical to the α-AlFeSi phase observed in our previous studies of rapidly solidified Al-Fe-V-Si alloys.[17,18]

Figure 6(a) shows a bright field TEM micrograph of the as-cast SC6061Mn alloy strip. It shows that the grain boundaries are again decorated by particles, as in the case of the as-cast SC6061 alloy strip. Microdiffraction and EDS analyses again show that they consist of Si particles and clusters of fine α-AlFe(Mn)Si particles. It can also be seen that the Al matrix of SC6061Mn alloy strip contains a larger volume fraction of

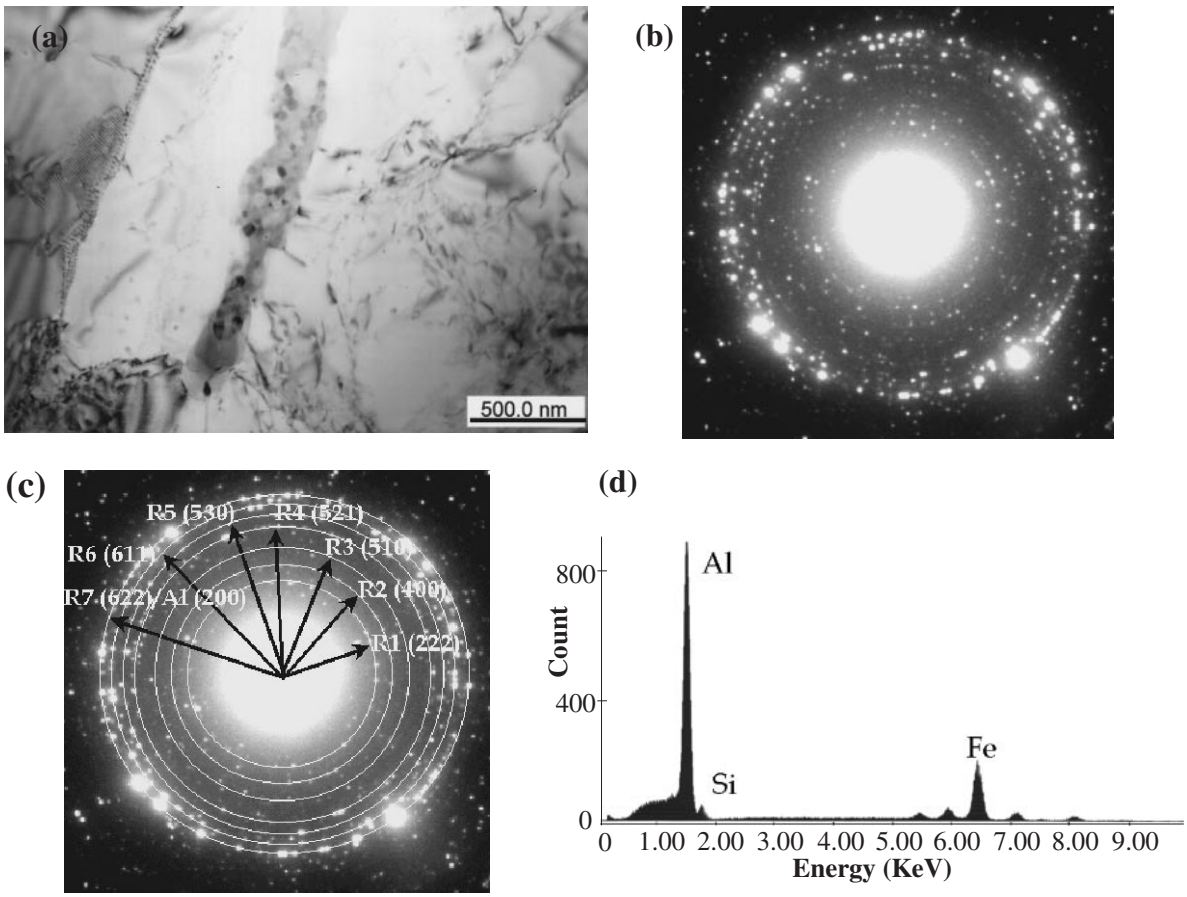

Fig. 5 (a) BF micrograph showing grain boundary particles in as-cast SC6061 alloy, (b) selected area diffraction pattern of grain boundary particles, (c) schematic drawing and indexing of selected area diffraction shown in (b), and (d) EDS spectra from grain boundary particles.

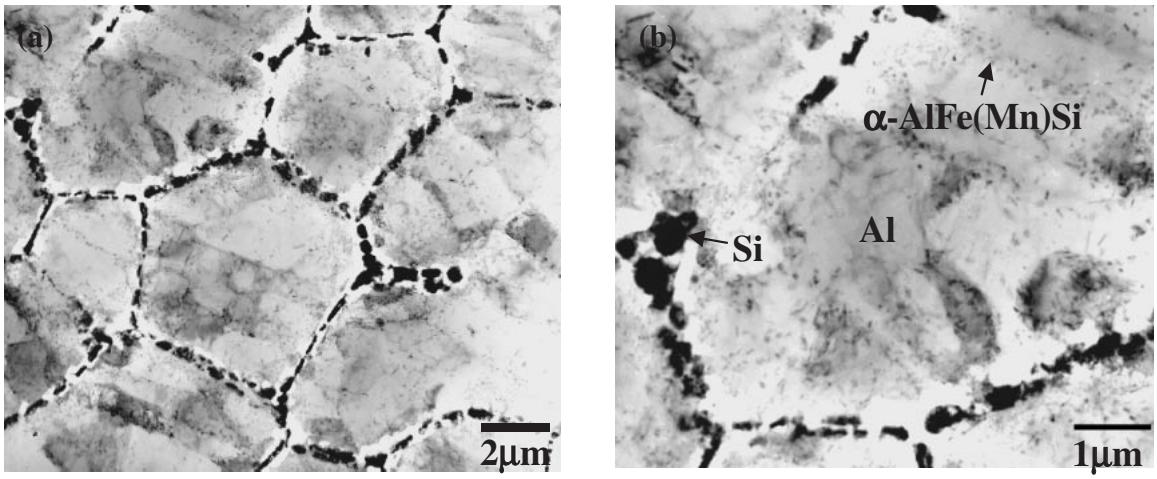

Fig. 6 (a) BF micrograph of as-cast SC6061Mn alloy and (b) magnified BF micrograph showing α-AlFe(Mn)Si particles within Al matrix.

fine particles (<100 nm) than that of SC6061 alloy strip (Fig. 6b). TEM analyses show that these fine particles are again α-AlFe(Mn)Si particles.

It is also interesting to note that there is the development of well-defined subgrains formed by recovery within the grain. During strip casting, solidified grains receive a large amount of rolling deformation. There can be an occurrence of recovery or recrystallization depending on the amount of deformation or the deformation temperature. The presence of a large amount of dislocations within the subgrains indicates that the temperature or the deformation was not enough for recrystallization to occur. These subgrains are more or less oriented parallel to the casting direction.

3.2.2 T6 Microstructure

Figure 7(a) shows the microstructure of a T6 treated (190°C for 2 h) SC6061 strip. Morphologically, the micro-

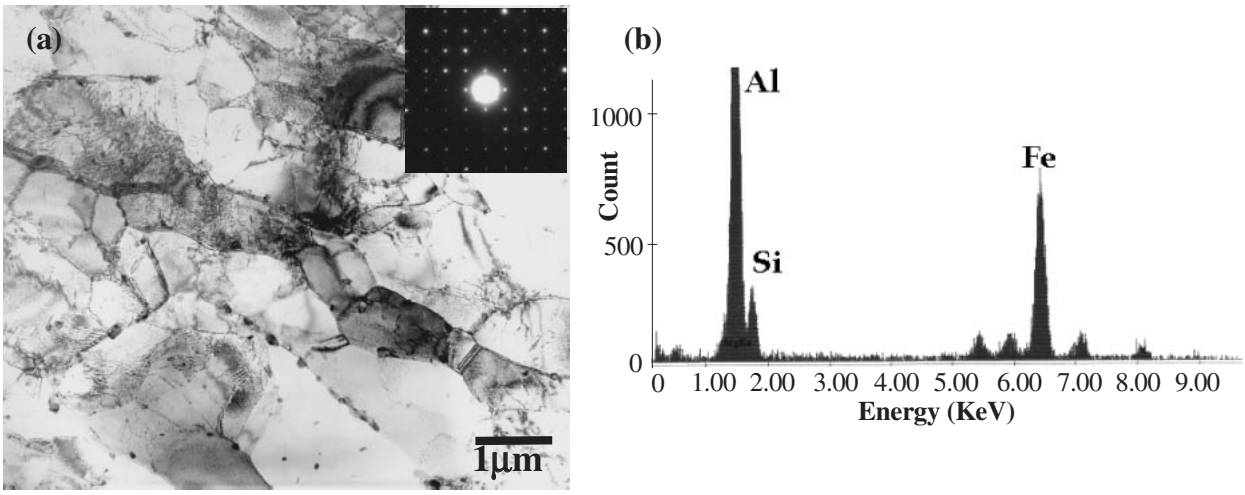

Fig. 7 (a) BF micrograph of T6 treated SC6061 alloy showing α-AlFeSi particles along grain boundaries and (b) EDS spectra from an α-AlFeSi particle.

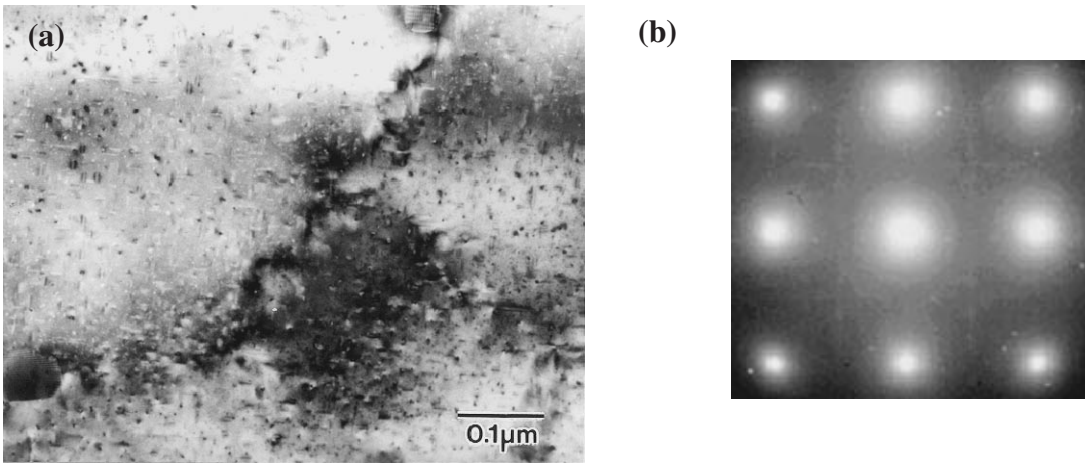

Fig. 8 (a) BF micrograph of T6 treated SC6061 alloy showing Mg_2Si particles within the Al matrix and (b) selected area diffraction pattern showing the streaks arising from Mg_2Si particles.

structure of the T6 treated specimen is quite similar to that of the as-cast specimen. However, there is a very important difference between these two specimens; the coarse Si particles present in the as-cast specimen have disappeared after heat treatment and are replaced by fine particles. Microdiffraction (insert in Fig. 7a) and EDS (Fig. 7b) analyses of the particles show that they are the α-AlFeSi phase. This suggests that Si particles dissolve and react with Al and Fe to form α-AlFeSi phase during heat treatment. One small but important difference between the microstructures of the as-cast and T6 treated specimens is that the α-AlFeSi particles in the latter have a more discrete form than those in the former. This indicates that there is a coalescence of the initially clustered α-AlFeSi particles into a thermodynamically stable polygonal form during heat treatment. There are also α-AlFeSi particles within the Al matrix, although their volume fraction is low. Besides the above mentioned α-AlFeSi particles, there is also a presence of very fine Mg_2Si particles within the Al matrix of the T6 treated SC6061 strip as shown in Figs. 8(a) and (b). In the Al-Mg-Si alloys, there are several types of precipitates such as GP zone, β'', β' and stable β, and peak strength is usually associated with the β'' and β'. It is known that the presences of β'' and β' in Al matrix give rise to streaks and satellite spots in SADP, respectively.[20–26] As shown in Fig. 8(b), SADP contains both streaks and satellite spots, indicating that Mg_2Si particles present in the T6 treated SC6061 strip are mixture of β'' and β'.

T6 heat treatment (180°C for 2 h) of the SC6061Mn alloy results in a similar microstructure to that of the base alloy. As shown in Fig. 9(a), however, there is a larger volume fraction of second phase particles within the matrix in the SC6061Mn alloy than in the SC6061 alloy. These particles have the same crystal structure as α-AlFeSi particles observed in the SC6061 alloy but contain Mn besides Al, Si and Fe as shown in Fig. 9(b). Comparison of the as-cast and T6 treated SC6061Mn specimens shows that the volume fraction and size of α-AlFe(Mn)Si particles increase by T6 heat treatment. It can also be seen that there are some particles which are rod-shaped, however, diffraction analysis shows that these particles are also α-AlFeSi particles. Although such types of particles are known to be detrimental to mechanical properties due to their asymmetric morphology, it might not be the case in the present study since they exist as fine particles. Figure 10 shows the bright field micrograph and

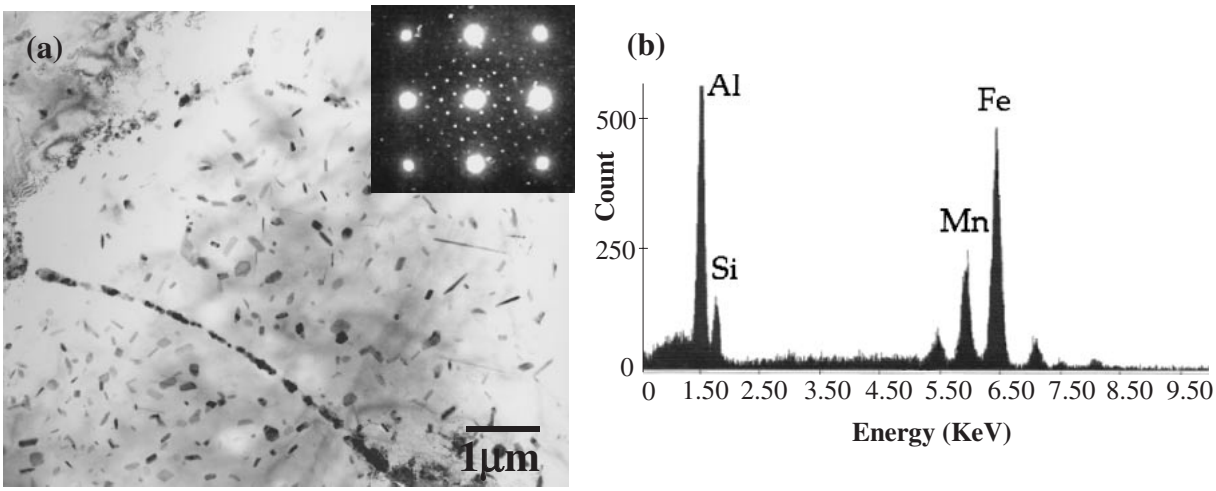

Fig. 9 (a) BF micrograph of T6 treated SC6061Mn alloy showing α-AlFe(Mn)Si particles along grain boundaries and within the Al matrix and (b) EDS spectra from an α-AlFe(Mn)Si particle.

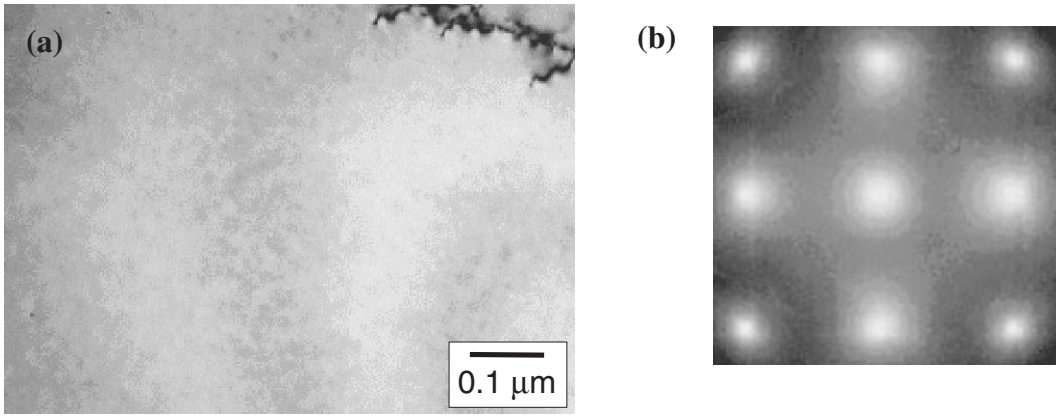

Fig. 10 (a) BF micrograph of T6 treated SC6061Mn alloy showing Al matrix and (b) selected area diffraction pattern.

SADP of Al matrix of the SC6061Mn alloy. The SADP shows the absence of streaking and satellite spots, indicating that the volume fraction of Mg_2Si particles in the T6 treated SC6061Mn alloy is very small. This is mainly due to the fact that the SC6061Mn alloy contains a larger volume fraction of α-AlFe(Mn)Si particles than the SC6061 alloy, thereby decreasing the amount of Si available for the formation of Mg_2Si particles during aging.

3.3 Mechanical properties

Figure 11 shows the variation of microhardness values of the strip cast alloys as a function of aging temperature when aged for 2 hours. It shows that the peak aging conditions are obtained at aging temperatures of 190°C and 180°C for the SC6061 alloy and the SC6061Mn alloy, respectively. It should be noted that the hardness of the SC6061Mn alloy is always lower than that of the SC6061 alloy at any aging temperature.

Table 2 shows the tensile properties of both strip cast alloys in the T6 treated condition. The tensile properties of the ingot cast and rolled commercial IM6061 alloy in the T6 treated condition are also shown for comparison purposes. The results show that the SC6061Mn alloy has a higher ultimate tensile strength than the SC6061 alloy with

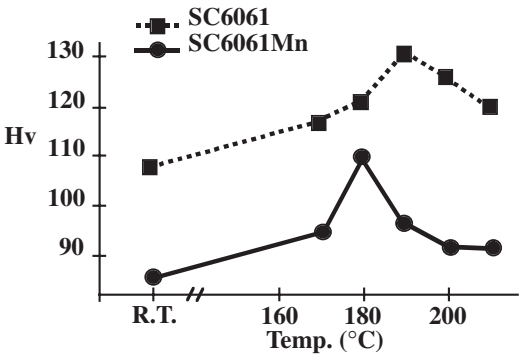

Fig. 11 Variation of microhardness values of SC6061 and SC6061Mn alloys with aging temperature (aging time: 2 hours).

Table 2 Tensile properties of the alloys used in the present study (T6 treated)

	YS (MPa)	UTS (MPa)	El. (%)
SC6061	197 ± 2	326 ± 1	23 ± 0.2
SC6061Mn	176 ± 1	350 ± 3	24 ± 0.4
IM6061	240 ± 1	330 ± 1	22 ± 0.2

equivalent elongation. The ultimate tensile strength of the SC6061 alloy is slightly lower than that of the IM6061 alloy, but the addition of Mn results in higher ultimate tensile strength and elongation than the IM6061 alloy. However, the yield strength values show a somewhat confusing behavior in that the yield strength of the IM6061 alloy is the highest, followed by the SC6061 alloy and the SC6061Mn alloy.

As shown previously, the main difference in the microstructure between the SC6061 alloy and the SC6061Mn alloy is a larger volume fraction of Mg_2Si particles and a smaller volume fraction of α-AlFe(Mn)Si particles in the former than in the latter. Although the exact contribution of each phase to the overall strength of the strip cast alloys is not known, it is expected that the yield strength of the strip cast alloys is mainly controlled by the more densely populated Mg_2Si particles. Therefore, the SC6061 alloy, which has a larger volume fraction of Mg_2Si particles, shows higher yield strength than the SC6061Mn alloy. The same can be said for the difference in the hardness values between the SC6061 and the SC6061Mn alloys. It shows that the SC6061Mn alloy has higher ultimate tensile strength with equivalent elongation than the SC6061 alloy despite its lower yield strength. Analysis of the stress-strain curves (Fig. 12) shows that the SC6061Mn alloy has a higher work hardening rate than the SC6061 alloy. This is undoubtedly due to a larger volume fraction of α-AlFe(Mn)Si particles in the SC6061Mn alloy than in the SC6061 alloy. Unlike the Mg_2Si particles which are susceptible to shearing by dislocations, α-AlFe(Mn)Si particles are incoherent with Al matrix[18,27,28] and thus induce the bypassing of dislocations.[29] In general, shearable precipitates do not contribute to work hardening significantly since there is no multiplication of dislocations around precipitates. Rather, they often cause severe planar slip. On the other hand, non-shearable dispersoids significantly contribute to work hardening since there is multiplication of dislocations around dispersoids. Hence the SC6061Mn alloy shows a higher work hardening rate and accordingly a higher ultimate tensile strength than the SC6061 alloy. The above discussion can also explain the lower yield strength of the strip cast alloys than that of the conventional IM alloy. The conventional IM alloy has a smaller volume fraction of α-AlFeSi particles and accordingly a larger volume fraction of Mg_2Si particles. Hence, the conventional IM alloy has a higher yield strength than the strip cast alloys.

As mentioned previously, the content of Fe is generally minimized in Al alloys since it forms various types of coarse intermetallic particles that have a deleterious effect on mechanical properties. However, Fe containing α-AlFeSi particles formed in the present alloy strip are finely distributed. Our previous studies[15,18] show that the α-AlFeSi phase is quite thermally stable and shows a high resistance to coarsening at elevated temperatures. It is worth noting that the α-AlFe(Mn)Si particles have a beneficial effect on the mechanical properties of the present strip cast alloys. In fact, improved high temperature properties of the rapidly solidified Al8009 alloy are due to the presence of finely distributed α-AlFe(Mn)Si particles.[30] The presence of these thermally stable α-AlFe(Mn)Si particles along grain boundaries restrict grain growth of the strip cast alloys during heat treatment, which results in a fine grain structure being retained.

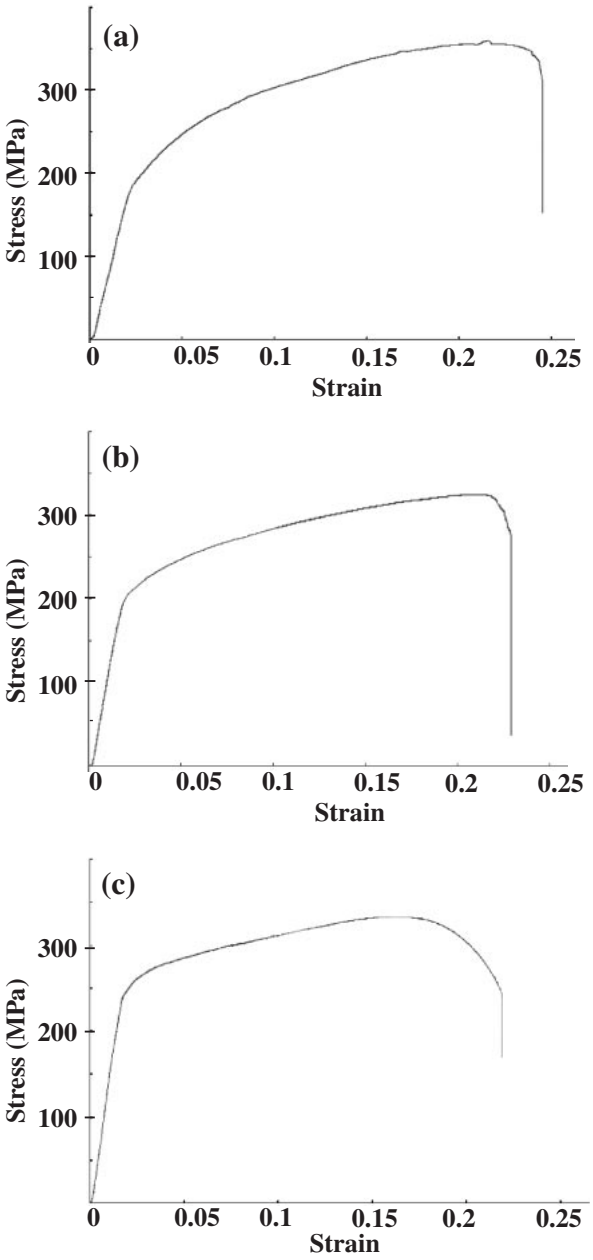

Fig. 12 Representative stress-strain curve of T6 treated specimens; (a) SC6061Mn alloy, (b) SC6061 alloy and (c) commercial IM6061 alloy.

4. Summary

The microstructure and mechanical properties of strip cast SC6061 alloy have been investigated. The effect of a Mn addition to the base alloy has also been investigated. The main conclusions from this study are as follows.

(1) The microstructure of the strip cast alloys in as-cast condition consists of a fine grained structure with Si particles along the grain boundaries. Within the grains, there is a development of dislocation subgrains which are the result of hot rolling during strip casting.

(2) By T6 heat treatment, Si particles along grain boundaries are replaced by fine α-AlFeSi particles. There is also a formation of α-AlFeSi particles within the Al matrix by heat treatment. The addition of Mn results in an increase in the volume fraction of α-AlFe(Mn)Si

particles within the Al matrix.

(3) Besides the α-AlFeSi type particles, there is also a precipitation of Mg_2Si particles within the Al matrix of both alloys. It has been shown that the base alloy contains a larger volume fraction of Mg_2Si precipitates than the Mn containing alloy.

(4) The base alloy has higher yield strength but lower ultimate tensile strength than the Mn containing alloy. The Mn containing alloy shows a much higher work hardening rate than the base alloy due to the presence of α-AlFe(Mn)Si dispersoids in the Al matrix of the former.

Acknowledgments

This work was supported by the 2003 National Research Laboratory (NRL) Program and the Center for Advanced Materials Processing (CAMP) of the 21st Century Frontier R&D Program Funded by the Ministry of Science and Technology, Korea.

REFERENCES

1) B. Frishchknech and K. P. Maiwald: *Light Metals 1988*, ed. by L. G. Boxall, (TMS, Warrendale, PA, 1988) p. 369.
2) H. D. Merchant, T. Z. Kattamis and J. G. Morris: *Continuous Casting of Non Ferrous Metals and Alloys*, eds. by H. D. Merchant, D. E. Taylor and E. H. Chia, (TMS, Warrendale, PA, 1989) p. 1-66.
3) L. O. Hazalden, G. J. Geiast and B. A. Parker: in Ref. 2), p. 163-176.
4) J. V. Wood: Mater. Sci. Technol. **4** (1988) 189-193.
5) T. W. Clyne: Met. Technol. **112** (1984) 350-355.
6) K. Shibuya and M. Ozawa: ISIJ Int. **31** (1991) 661-668.
7) A. R. Buchner and J. W. Schmitz: Steel Res. **62** (1991) 346-351.
8) N. Tsuji, K. Tsuzaki and T. Maki: ISIJ Int. **32** (1992) 1319-1328.
9) P. Vangala *et al.*: *Melt-spinning and Strip Casting*, ed. by E. F. Matthys, (TMS, Warendale, PA, 1992) p. 225.
10) H. Yasunaka: ISIJ Int. **35** (1995) 784-789.
11) A. L. Robson, G. L. Thompson, P. Longdon and A. Wilkinson: *Thermec 97*, ed. by T. Chandra, (TMS, Warrendale, PA, 1997) p. 2263.
12) C. J. Petry: *Aluminum Alloys - Physical and Mechanical Properties*, eds. by E. A. Starke, Jr. and T. H. Sanders, Jr., (EMAS, U. K., 1986) p. 111.
13) E. A. Loria: *Aluminum Alloys - Physical and Mechanical Properties*, eds. by E. A. Starke, Jr. and T. H. Sanders, Jr., (EMAS, U. K., 1986) p. 133.
14) Y. Saito, N. Tsuji, Y. Nagai and S. Takai: *Thermec 97*, ed. by T. Chandra, (TMS, Warrendale, PA, 1997) p. 2381.
15) H. J. Koh and N. J. Kim: J. Kor. Inst. Met. & Mater. **36** (1998) 2027-2034.
16) H. J. Koh and N. J. Kim: J. Kor. Inst. Met. & Mater. **36** (1998) 2035-2042.
17) H. J. Koh, W. J. Park and N. J. Kim: Mater. Trans., JIM **39** (1998) 982-988.
18) W. J. Park, S. Ahn and N. J. Kim: Mater. Sci. Eng. A**189** (1994) 291-299.
19) N. J. Grant: *Rapid Solidification Processing*, eds. by R. Mehrabian, B. H. Kear and M. Cohen, (Baton Rouge, LA, Claitor Publishing Division, 1970) p. 230.
20) M. H. Jacobs: Philos. Mag. **26** (1972) 1-13.
21) K. Matsuda, S. Ikeno and S. Tada: J. Japan Inst. Metals **57** (1993) 1107-1113.
22) G. A. Edwards, K. Stiller, G. L. Dunlop and M. J. Couper: Acta Mater. **46** (1998) 3893-3904.
23) K. D. Woo, J. S. Lee and S. W. Kim: Metals and Materials **5** (1999) 363-368.
24) M. Murayama and K. Hono: Acta Mater. **47** (1999) 1537-1548.
25) H. K. Ahn and C. H. Yu: Metals and Materials International **7** (2001) 1-7.
26) M. Verwerft: Acta Mater. **48** (2000) 1097-1104.
27) N. J. Kim: Int. J. Rapid Solidification **6** (1991) 175-184.
28) D. J. Skinner, R. L. Bye, D. Raybould and A. M. Brown: Scr. Metall. **20** (1986) 867-872.
29) I. S. Kim, N. J. Kim and S. W. Nam: Scr. Metall. **32** (1995) 1813-1819.
30) S. Lee, D. Y. Lee and N. J. Kim: Mater. Sci. Eng. A **147** (1991) 33-44.